

This discussion paper is/has been under review for the journal Atmospheric Measurement Techniques (AMT). Please refer to the corresponding final paper in AMT if available.

Application of bias correction methods to improve the accuracy of quantitative radar rainfall in Korea

J.-K. Lee¹, J.-H. Kim², and M.-K. Suk²

¹Innovation Center for Engineering Education, Daejin University, Pocheon-si, Gyeonggi-do, Korea

²Weather Radar Center, Korea Meteorological Administration, Seoul, Korea

Received: 22 October 2015 – Accepted: 23 October 2015 – Published: 3 November 2015

Correspondence to: J.-K. Lee (myroom1@daejin.ac.kr)

Published by Copernicus Publications on behalf of the European Geosciences Union.

AMTD

8, 11429–11465, 2015

Application of bias correction methods to improve quantitative radar rainfall in Korea

J.-K. Lee et al.

[Title Page](#)

[Abstract](#)

[Introduction](#)

[Conclusions](#)

[References](#)

[Tables](#)

[Figures](#)

[◀](#)

[▶](#)

[◀](#)

[▶](#)

[Back](#)

[Close](#)

[Full Screen / Esc](#)

[Printer-friendly Version](#)

[Interactive Discussion](#)



Abstract

There are many potential sources of the biases in the radar rainfall estimation process. This study classified the biases from the rainfall estimation process into the reflectivity measurement bias and the rainfall estimation bias by the Quantitative Precipitation Estimation (QPE) model and also conducted the bias correction methods to improve the accuracy of the Radar-AWS Rainrate (RAR) calculation system operated by the Korea Meteorological Administration (KMA). In the Z bias correction for the reflectivity biases occurred by measuring the rainfalls, this study utilized the bias correction algorithm. The concept of this algorithm is that the reflectivity of the target single-pol radars is corrected based on the reference dual-pol radar corrected in the hardware and software bias. This study, and then, dealt with two post-process methods, the Mean Field Bias Correction (MFBC) method and the Local Gauge Correction method (LGC), to correct the rainfall estimation bias by the QPE model. The Z bias and rainfall estimation bias correction methods were applied to the RAR system. The accuracy of the RAR system was improved after correcting Z bias. For the rainfall types, although the accuracy of the Changma front and the local torrential cases was slightly improved without the Z bias correction the accuracy of the typhoon cases got worse than the existing results in particular. As a result of the rainfall estimation bias correction, the Z bias_LGC was especially superior to the MFBC method because the different rainfall biases were applied to each grid rainfall amount in the LGC method. For the rainfall types, the results of the Z bias_LGC showed that the rainfall estimates for all types was more accurate than only the Z bias and, especially, the outcomes in the typhoon cases was vastly superior to the others.

1 Introduction

Weather radars can provide rainfall estimates over the Korean Peninsula and near seas with high spatial (minimum 0.125 km) and temporal resolutions (2.5 min), and

AMTD

8, 11429–11465, 2015

Application of bias correction methods to improve quantitative radar rainfall in Korea

J.-K. Lee et al.

Title Page	
Abstract	Introduction
Conclusions	References
Tables	Figures
◀	▶
◀	▶
Back	Close
Full Screen / Esc	
Printer-friendly Version	
Interactive Discussion	



they play an important role in predicting and monitoring severe weather conditions. However, several sources of biases are involved in the process of calculating quantitative radar-based rainfall estimates. It is well acknowledged that radar data are affected by both systematic bias (due to reflectivity measurements that are included in hardware errors, signal processing, and quality controls, and parameter estimation of the $Z-R$ relationship, as well as quantitative precipitation estimation model structures) and random error (Huff, 1970; Woodely et al., 1957; Wilson and Brandes, 1979; Austin, 1987; Campos and Zawadzki, 2000; Krajewski and Smith, 2002) because one of major reasons is that weather radars indirectly measure rainfall amounts using the relationships between measured radar variables and observed rainfalls, such as $Z-R$, $Z_{DR}-R$, and $K_{DP}-R$. Related to systematic bias, a considerable number of studies have been conducted to correct the reflectivity measurement biases, which includes temporal and spatial sampling bias, ground and sea clutter, beam-blockage and attenuation, electrical calibration, and the quantification of the reflectivity bias (Chumchean et al., 2006). Jordan et al. (2000) evaluated the biases which arise in radar estimates of rainfall as a result of temporal sampling (spatial averaging), measuring the field at some distance above the ground, and recording the reflectivity data with a limited radiometric resolution. Germann et al. (2006) modified the ground clutter algorithm and reduced the amount of residual non-meteorological signals in a mountainous region (the Alps), to improve the precipitation estimation. Villarini and Krajewski (2008) investigated the spatial sampling errors in radar observations, which affect the sensitivity of the models, and determined that these errors were related to the approximation of an areal estimate by a using a point measurement. Similarly, converting the measured reflectivity to a rainfall amount using artificial relationships or models is one of the major sources of bias. To overcome these limitations, gauge adjustment methods were applied to correct misestimated precipitation, in numerous existing studies. Sinclair and Pegram (2005) described a merging technique and presented an application of it to a simulated rainfall field. The proposed merging technique, based on Conditional Merging (CM) (Ehret, 2002), made use of a Kriging method to reduce the bias while retaining

Application of bias correction methods to improve quantitative radar rainfall in Korea

J.-K. Lee et al.

[Title Page](#)

[Abstract](#)

[Introduction](#)

[Conclusions](#)

[References](#)

[Tables](#)

[Figures](#)

[◀](#)

[▶](#)

[◀](#)

[▶](#)

[Back](#)

[Close](#)

[Full Screen / Esc](#)

[Printer-friendly Version](#)

[Interactive Discussion](#)



5 spatial detail from the radar but keeping the spatial variability observed by the radar. Morin and Gagella (2007) compared three radar-gauge adjustment methods, a one-coefficient bulk adjustment, a Weighted Regression (WR), and a Weighted Multiple Regression (WMR), for the radar-based quantitative precipitation estimation over the
10 Mediterranean and dry climate regimes. They concluded that the WR and WMR adjustment methods were useful for calculating rain depth estimates, with some limitations. Goudenhoofdt and Delobbe (2009) dealt with several radar-gauge merging methods, considering the gauge network densities, and compared their precipitation estimates accuracy. The analysis revealed that the simple methods reduced the bias of radar estimation, and the geostatistical merging methods resulted in a better performance that reflected the gauge network densities.

15 Using a series of procedures which estimate the quantitative rainfalls derived from radar information, this paper focuses on correcting the measurement bias and the bias by the QPE model because the measurement and estimation procedures of rainfall play and important roles to the accuracy of weather radar rainfall. The measurement bias (hereafter Z bias) is defined as the only reflectivity measurement bias which occurs while using weather radar hardware systems to detect precipitation. The bias by the QPE model (hereafter rainfall estimation bias) is defined as the estimated rainfall-bias, which includes the bias due to the parameters of the $Z-R$ relationship, the parameters
20 of the QPE model, and the QPE model structure. Section 2 describes the correction methods of the Z bias and the rainfall estimation used in this paper. Section 3 gives results for the rainfall estimation, using the correction methods, and describes the effect of the Z bias and rainfall estimation bias correction methods. Finally, Sect. 4 summarizes the results and provides some concluding remarks.

Application of bias correction methods to improve quantitative radar rainfall in Korea

J.-K. Lee et al.

[Title Page](#)

[Abstract](#)

[Introduction](#)

[Conclusions](#)

[References](#)

[Tables](#)

[Figures](#)

[|◀](#)

[▶|](#)

[◀](#)

[▶](#)

[Back](#)

[Close](#)

[Full Screen / Esc](#)

[Printer-friendly Version](#)

[Interactive Discussion](#)

2 Data and methodology

2.1 Radar dataset and rainfall cases

In this study, the performance of the bias correction methods has been evaluated by comparing the observed rainfall data from rain gauges operated by the KMA (Korea Meteorological Administration). The observed rainfall data were collected from 642 ground rain gauges (called AWS, Automatic Weather Station) located in the Korean Peninsula, 321 of which were for calibration, and 321 for validation in Fig. 1. The Bilsan S-band dual-polarimetric radar, which was installed and operated by the Ministry of Land, Infrastructure and Transport (MLIT) in 2009, was selected to be the absolute reference radar to estimate the Z bias (described in Sect. 2.2). Horizontal and vertical reflectivity (Z_H and Z_V), differential reflectivity (Z_{DR}), differential phase (Φ_{DP}), specific differential phase (K_{DP}), correlation coefficient (ρ_{HV}), and spectrum width (SW) were estimated with a gate size of 0.125 km. The scan strategy has six elevation angles, with a 2.5 min update cycle. The Accuracy of a reference radar shows that bias is 2.01 mm h^{-1} , RMSE is 3.55 mm h^{-1} , and correlation coefficient is 0.89 in 10 rainfall cases from October 2011 to October 2012. Other studies also show a reference radar has more than 80 % accuracy, on average, in both quantitative and qualitative tests (You et al., 2014; Jeong et al., 2014; Kim et al., 2015). The target radars that required Z bias correction were 11 single-polarimetric radars (Baegnyeondo, Kwanaksan, Oseonsan, Jindo, Gosan, Seongsan, Gudeoksan, Myeonbongsan, Gangneung, Gwnagdeoksan, Incheon) with a scan range of maximum 200 km (C-band) and 240 km (S-band), and a gate size of 0.250 km, operated by the KMA, in Fig. 2. Table 1a shows the radars and rain-gauges used for estimating the Z bias and the data period, and Table 1b shows the 18 rainfall cases (in the summer season) used for the verification of the Z bias and rainfall estimation bias correction methods.

Title Page

Abstract

Introduction

Conclusions

References

Tables

Figures

◀

▶

◀

▶

Back

Close

Full Screen / Esc

Printer-friendly Version

Interactive Discussion

2.2 Quantitative precipitation estimation model

This paper utilized the Radar-AWS Rainrate (RAR) calculation system (Hereafter called the RAR system) for the QPE model. The RAR system, which was developed by the KMA in 2006, is operated on site, based on 11 single-polarimetric radars. The RAR system produces a merged rainfall field for the Korean Peninsula through a series of steps (production of the radar reflectivity field, calculation of AWS rainfalls, derivation of the $Z-R$ relationship, etc.) (refer to Fig. 3).

The RAR system estimates the parameters of the $Z-R$ relationship, in real-time, for real-time rainfall estimates (Weather Radar Center, 2011). The RAR system utilizes 10 min reflectivity and AWS rainfall, in the Window Probability Matching Method (WPMM) (Rosenfeld et al., 1993), to estimate the rainfalls in each radar site and the merged rainfalls of radar sites for producing composite rainfall fields. The used reflectivity, which are quality controlled (removal of non-meteorological echoes), are averaged on 3×3 pixels with a certain AWS as the centers are used. The WPMM method reproduces the probability density functions (pdfs) of ground rainfall from the AWSs, and radar reflectivity, and determines the $Z-R$ relationship using these pdfs (refer to Eqs. 1 and 2) (Rosenfeld et al., 1993).

$$\int_0^{\infty} f(Z_e) P_c(Z_e) dZ_e = \int_0^{\infty} R P_c(R) dR \quad (1)$$

$$P_c(R) = P(R|R > R_T), \quad P_c(Z_e) = P(Z_e|Z_e > Z_{eT}) \quad (2)$$

where Z_e is the radar reflectivity (dBZ), $P_c()$ is the conditional probability function, R is the rainfall (mm h^{-1}), and T is the threshold.

The conditional probability functions in Eq. (1) are derived from Eq. (2), and the thresholds of rainfall and radar reflectivity are 0.1 mm h^{-1} and 10 dBZ . The parameters of the $Z-R$ relationship have been estimated using radar reflectivity and AWS rainfalls, from 1 prior, with the least square fit of the power law. The number of radar reflec-

Title Page

Abstract

Introduction

Conclusions

References

Tables

Figures

|◀

▶|

◀

▶|

Back

Close

Full Screen / Esc

Printer-friendly Version

Interactive Discussion

tivity and AWS rainfalls over a certain threshold are required in order to estimate the parameters accurately. If there is not enough data, the estimated rainfalls from that $Z-R$ relationship are inaccurate. To overcome this limitation, if the number of available AWSs is more than 30 % of those available in each radar site, the parameters of the 5 $Z-R$ relationship can be estimated. If it is less than 30 %, $Z = 200R^{1.6}$ (Marshall and Palmer, 1948) is applied for the rainfall estimates (Korea Meteorological Administration, 2012b).

Secondly, the composite rainfall field for the whole country may be produced using each radar rainfall estimate; however, appropriate merging methods (including maximum value, average value, minimum value, and distance weighting methods) must be conducted because the scan ranges of the radar sites overlap. Because the maximum value method is applied to merge radar rainfalls by the KMA (Korea Meteorological Administration, 2012b), the identical method is also utilized in this paper.

2.3 Bias correction methods

15 2.3.1 Reflectivity measurement bias correction method

Weather radars continuously carry out measurement cycles, which include sending signals into the atmosphere and receiving and analyzing the return signals for meteorological observation. The measurement of the reflectivity itself suffers from hardware malfunctions (e.g. electronic miscalibration, signal misprocessing) and radar characteristics (e.g. attenuation). When converting radar reflectivity into rainrates ($Z-R$ relationship) leads to an additional bias that can lower the accuracy of rainfall estimation. To estimate the Z bias of the target weather radars, a reference weather radar that has been absolutely corrected is required. The Z bias is defined as the difference between the measured reflectivity of the reference radar and the target radar, under the 20 same spatial and temporal conditions (Weather Radar Center, 2012). The procedure of estimating the Z bias is described as follows.

[Title Page](#)[Abstract](#)[Introduction](#)[Conclusions](#)[References](#)[Tables](#)[Figures](#)[◀](#)[▶](#)[◀](#)[▶](#)[Back](#)[Close](#)[Full Screen / Esc](#)[Printer-friendly Version](#)[Interactive Discussion](#)

This paper selected a Bislsan S-band dual-polarimetric radar (hereafter Bislsan dual-pol radar), which can be self-calibrated and is more accurate than the reference weather radar. To calibrate the Bislsan dual-pol radar, a self-consistency constraint method that uses the relationship between the reflectivity (Z), varied by the radar beam power and the specific differential phase (K_{DP}) and affected by only the particle size or the concentration and not the radar beam power, was utilized. The procedure of the self-consistency constraint method is as follows (Weather Radar Center, 2012).

1. Derive the Z_H – K_{DP} relationship, theoretically, from the Drop Size Distributions (DSDs).
10
2. Calculate the K_{DP} for each radar pixel from the observed Z_H , using the derived Z_H – K_{DP} relationship and the Φ_{DP} as the integrating calculated K_{DP} along each radial.
15
3. Calculate the difference angle (θ) using a scatter plot between the calculated Φ_{DP} , from (2) and observed from the Bislsan dual-pol radar, and calculate the Z bias (ε) by inputting the difference angle (θ) into Eqs. (3) and (4) (Lee et al., 2006) (refer to Fig. 4).

$$\tan \theta = \frac{\sum_{i=1}^n (\Phi_{DP_cal} - \Phi_{DP_obs})}{\sum_{i=1}^n \Phi_{DP_obs}^2} \quad (3)$$

$$\varepsilon(\text{dB}) = 10b \log(\tan \theta) \quad (4)$$

- 20 where, Φ_{DP_cal} is the theoretical Φ_{DP} from the DSDs, Φ_{DP_obs} is the observed Φ_{DP} from the dual-pol radar, θ is the difference angle, b is the empirical constant, and ε is the estimated Z bias.

Application of bias correction methods to improve quantitative radar rainfall in Korea

J.-K. Lee et al.

[Title Page](#)

[Abstract](#)

[Introduction](#)

[Conclusions](#)

[References](#)

[Tables](#)

[Figures](#)

[|◀](#)

[▶|](#)

[◀](#)

[▶](#)

[Back](#)

[Close](#)

[Full Screen / Esc](#)

[Printer-friendly Version](#)

[Interactive Discussion](#)

After calibration of the Bislsan dual-pol radar for the Z bias was completed, the target single-pol radars that are located adjacent to the reference radar were calibrated according to the reflectivity of the reference radar. The procedure for calculating the Z bias of the target radars is as follows (Korea Meteorological Administration, 2011).

1. Remove the beam-blockage area using the beam-blockage information (penetration ratio more than 90 %).
2. Reflect the accumulated attenuation effects, due to the rainfall, in the observed reflectivity (attenuation ratio less than 10 %).
- 10 3. Generate the 3-dimensional CAPPI for the reflectivity.
4. Set up equidistant pairs between the reference and target radars, within 200 km from the center of the reference radar; however, whenever a Bislsan dual-pol radar was the reference radar, the distance was within 100 km.
- 15 5. Compare the reflectivity of the reference and target radars, within a ± 5 km reflectivity overlap area.
6. Calculate the reflectivity differences, at intervals of 0.5 km from 1.5–3.5 km altitude, with consideration to the ground clutter and the bright band, and average the reflectivity differences for the Z bias of the target radar.

Figure 5 shows the concept of the Z bias for the target radar, which has been calculated from the reflectivity differences in the overlap area, between the reference and the target radars. After the calibration of the target radar #1 for the Z bias was completed, target radar #1 was the reference radar for target radar #2 (adjacent to target radar #1). The procedure mentioned above was equally applied for target radar #1 and #2, to calculate the Z bias of target radar #2.

[Title Page](#)

[Abstract](#)

[Introduction](#)

[Conclusions](#)

[References](#)

[Tables](#)

[Figures](#)

[◀](#)

[▶](#)

[◀](#)

[▶](#)

[Back](#)

[Close](#)

[Full Screen / Esc](#)

[Printer-friendly Version](#)

[Interactive Discussion](#)

2.3.2 Rainfall estimation bias correction methods

The estimated rainfall, based on the radars, has the QPE model bias (parameters of $Z-R$ relationship, parameters of QPE model, QPE model structures, etc.) even if calibrated reflectivity is inputted into the QPE model. In this paper, the Mean Field Bias

5 Correction (MFBC) method and the Local Gauge Correction (LGC) method have been applied to the outcomes from the QPE model, in order to correct the rainfall estimation bias.

Mean field bias correction method

The fundamental concept of the MFBC method is that the bias correct factor (G/R ratio

10 factor) is calculated using the ratio of the spatial average (mean), between the rainfalls, estimated using radars and observed rainfall at a corresponding field (or point, pixel). Then corrected rainfall is calculated by multiplying the G/R ratio factor, and the radar rainfall estimates. The equation of the MFBC method is as follows.

$$G/R \text{ ratio factor} = \frac{\sum_{i=1}^n G_i}{\sum_{i=1}^n R_i} \quad (5)$$

15 where, G_i is the rainfall of the i th rain gauge, R_i is the radar rainfall estimates of the i th point (or pixel), and n is the total number of the ground rain gauge. In the case of utilizing the MFBC method in a certain area (or for a certain period), the identical G/R ratio factor is uniformly applied to radar rainfall estimates all over the area.

Local Gauge Correction method

20 This study dealt with the Local Gauge Correction (LGC) method, which has been employed in the NMQ (National Mosaic and QPE) of the NOAA (National Oceanic and Atmospheric Administration) and NSSL (National Severe Storms Laboratory) (Zhang et al., 2011). The LGC method, which assigns the weights to a bias between the ground

[Title Page](#)

[Abstract](#)

[Introduction](#)

[Conclusions](#)

[References](#)

[Tables](#)

[Figures](#)

[◀](#)

[▶](#)

[Back](#)

[Close](#)

[Full Screen / Esc](#)

[Printer-friendly Version](#)

[Interactive Discussion](#)

rainfall detected by AWSs and the radar rainfall estimates, is a modified version of the Inverse Distance Weighting (IDW) method. The LGC method is able to correct the rainfall cases that occur locally by modifying the rainfall estimates in each pixel. The procedure of the LGC method is as follows (refer to Fig. 6):

5 This paper defined that $r_{\text{LGC},i}$ is the corrected rainfall estimates in a certain point i , r_i is the radar rainfall estimates in a certain radar pixel i , and $R_{e,i}$ is the expected error estimates. This relationship is expressed as following equation:

$$\text{STEP 1: } r_{\text{LGC},i} = r_i - R_{e,i} = r_{\text{LGC},i}(b, D) \quad (6)$$

where D is the effective radius for calculating the radar rainfall bias, b is the weight of the variable d , and d is the distance between the AWSs and the pixels in the radars. The estimated weights, according to Eq. (7), are applied to Eq. (6) (Zhang et al., 2011).

$$R_{e,i} = \sum_{j=1}^m e_j w_j / \sum_{j=1}^m w_j \quad (7)$$

If general, $w_j = 1/d_j^b$ (if $d_j \leq D$) or 0 (if $d_j > D$)

If the numbers of AWS in the region are sparse,

$$15 \quad \alpha = \sum_{j=1}^m \exp \left[-d_j^2 / (D/2)^2 \right]; \quad w_j = \alpha \times 1/d_j^b \text{ (if } d_j \leq D \text{) or 0 (if } d_j > D \text{)} \quad (8)$$

where e_j is the error between the rainfalls observed from the AWSs (g_j) and the radar rainfall estimates (r_j), w is the weight of the error ($= r_j - g_j$), j is the j th AWS, m is the number of AWSs within the effective radius, and α is the impact factor. If the α is more than one, the number of AWSs is enough for the rainfall-bias correction. Otherwise, if it is less than one, if the number of AWSs is sparse (the α is less than one), the revised weights have been calculated by multiplying α with the original weights ($w_j = \alpha \times 1/d_j^2$).

Title Page

Abstract

Introduction

Conclusions

References

Tables

Figures

|◀

▶|

◀

▶

Back

Close

Full Screen / Esc

Printer-friendly Version

Interactive Discussion

E_i is defined as the difference between the r_{LGC} from STEP 1 and the ground rainfall, g_i , and it depends on b and D .

STEP 2: $E_i = r_{\text{LGC}} - g_i = E_i(b, D)$ (9)

The Mean Square Error (MSE) for E_i is expressed as Eq. (10), and it also depends on parameters b and D . The parameters of the LGC method (b and D) have been determined using the stepwise method for minimizing the MSE value, and applied to Eq. (8) to calculate the radar rainfall estimates, r_{LGC} .

STEP 3: $\text{MSE} = \sum_{i=1}^n E_i^2 / n = \text{MSE}(b, D)$ (10)

This paper has assumed that the scan range of the radars (D) is the maximum range (240 km) used by all AWSs on the Korean Peninsula. Although it takes a long time to carry out the LGC algorithm under this assumption, it is considered to be appropriate to verify the improvement of the radar rainfall estimates using the LGC method.

In sequence, because the LGC method is highly dependent on the number of AWSs that are available and accurate, a quality control algorithm for the AWSs has been conducted to remove lower-quality AWSs that have larger expected errors than the others. The conditions of the quality control are as follows: (i) in a certain AWS, if the number of pixels that have a $D_{R,E}$ less than 5 mm are less than 25 % of the total pixels, a certain AWS is designated as an “abnormal AWS” and is thus removed. $D_{R,E}$ are the differences between $R_{e,i}$ and E_i , within 10 km radius from the center of a certain AWS. (ii) The LGC method has been conducted until the number of available AWSs was more than 90 % of all the filtered AWSs. If this procedure is stopped, a calculated r_{LGC} at the present stage is used for the corrected rainfall estimates. (iii) The procedure of the LGC method is finally finished after repeating the routine more than approximately four times. Furthermore, if the ratio of the abnormal AWSs is more than 7 %, the procedure of the LGC method is also finished (Korea Meteorological Administration, 2012).

Title Page

Abstract

Introduction

Conclusions

References

Tables

Figures

◀

▶

◀

▶

Back

Close

Full Screen / Esc

Printer-friendly Version

Interactive Discussion

The thresholds were decided using the stepwise method, and are appropriate for the LGC method applied to the RAR calculation system. However, since the thresholds are somewhat subjective, it is considered that future studies should be conducted that deal with this limitation.

5 3 Application and results

3.1 Application of the reflectivity measurement bias correction method

In Sect. 2.2.1, the reflectivity measurement bias (Z bias) for the Bislsan dual-pol radar have been estimated using the self-consistency constraint method that employs the relationship between reflectivity (Z) and a specific differential phase (K_{DP}) during the calibration period. The Z bias of the Bislsan dual-pol radar was estimated to be -2.61 dB, with the result that the calculated $\tan\theta$ (which was 0.58° from Eq. 1) was inputted into Eq. (4). The Bislsan dual-pol radar was self-calibrated, using its Z bias. For estimating the Z bias of the target radars, first of all, the pairs between the reference radar and the target radar were set up (refer to Table 2). Then, the averaged Z biases of the 11 single-pol radars operated by the KMA, as the target radars were estimated sequentially from the beginning using the Bislsan dual-pol radar as the reference radar (refer to Fig. 7 and Table 3). The Z biases of the BRI and the JNI sites were -7.87 dB (the largest) and -1.16 dB (the smallest) and the Z bias, on average, was -4.52 dB. The radar rainfall estimates, in particular, were underestimated due to the fact that all of the Z biases had negative values.

To verify the improvement of the radar rainfall estimates, the RAR system, which reflected the Z biases of all the radar sites, was used to calculate the rainfall estimates of 18 cases in the summer season. In Fig. 8, after applying the Z biases to the RAR system, the accuracy of the rainfall estimates improved in the Root Mean Square Error (RMSE) and the correlation coefficient, which ranged from 7.37, 0.83, 7.21, and 0.84 mm h^{-1} on average, respectively. As a result of each rainfall type, in the RMSE,

Title Page

Abstract

Introduction

Conclusions

References

Tables

Figures

◀

▶

Back

Close

Full Screen / Esc

Printer-friendly Version

Interactive Discussion

the accuracy of the rainfall estimates in the Changma front cases improved from 7.43 to 7.36 mm h^{-1} , and the accuracy of local torrential rainfall cases (7.43 mm h^{-1}) was similar to the results without the application of the Z bias (7.36 mm h^{-1}). In particular, the accuracy of typhoon cases deteriorated compared to the existing results (from 9.08 to 11.04 mm h^{-1}). This was due to the application of Z biases to each radar site in the RAR system, which has increased the rainfall estimates for the whole country. The accuracy of Changma front cases, which occur nationwide, was improved. However, because the cases of local torrential rainfalls and typhoons occurred locally, the accuracy of these cases was negatively impacted. In Fig. 9a, in Case 12 at 15:00 LST on 10 August 2012, the image before the application of the Z bias is shown, and Fig. 9b shows the image after the Z bias correction. The rainfall estimates, in the black dash circles on the partial magnification image in Fig. 9b, are stronger than those in Fig. 9a, since the rainfall estimates were increased by the Z bias correction. It has been proven that the Z bias correction proposed by this paper has improved the accuracy of the rainfall amounts in the RAR system.

3.2 Application of the rainfall estimation bias correction methods

Since the rainfall estimates in the RAR system were improved by the Z bias correction in Sect. 3.1, the rainfall estimation bias correction methods were conducted after the Z bias correction. To verify the improvement of the radar rainfall amounts estimated by the rainfall estimation bias correction, the RAR system (with the rainfall-bias correction) was conducted for 18 summer season cases over the verification period. This paper defined that the results with only the Z bias correction were identified as “ Z bias”, the results with the Z bias correction and the MFBC method were identified as “ Z bias_MFBC”, and the results with the Z bias correction and the LGC method were identified as “ Z bias_LGC”.

As a result of the rainfall estimation bias correction methods, Table 4 shows the accuracy of the rainfall estimates for each rainfall estimation bias method and each rainfall type. In Table 4a, Mean Absolute Error (MAE) of the Z bias, Z bias_MFBC,

Application of bias correction methods to improve quantitative radar rainfall in Korea

J.-K. Lee et al.

[Title Page](#)

[Abstract](#)

[Introduction](#)

[Conclusions](#)

[References](#)

[Tables](#)

[Figures](#)

[|◀](#)

[▶|](#)

[◀](#)

[▶](#)

[Back](#)

[Close](#)

[Full Screen / Esc](#)

[Printer-friendly Version](#)

[Interactive Discussion](#)

and Z bias_LGC were 3.65, 3.37, and 2.19 mm h^{-1} , respectively. Among them, the accuracy of the Z bias_LGC was superior to the others. In the RMSE, the accuracy of the rainfall amounts of the RAR system was improved by about 7.4% (from 7.21 to 6.68 mm h^{-1}) in the Z bias_MFBC and 63.7% (from 7.21 to 2.62 mm h^{-1}) in the Z bias_LGC. In the correlation coefficient, the accuracy of the RAR system was also improved by about 10.7% (from 0.84 to 0.93) in the Z bias_MFBC and 11.7% (from 0.84 to 0.94) in the Z bias_LGC. It is proven that the accuracy of the rainfall estimates in the RAR system was improved by the Z bias with the rainfall estimation bias correction methods more than only the Z bias. Especially, among the rainfall estimation bias correction methods, the Z bias_LGC is superior to the others; the reason for this is that although the same rainfall estimation bias was applied to the overall application region in the MFBC method, different rainfall estimation biases were applied to each rainfall amount by the radar pixel in the LGC method. In Table 4b, although the correlation coefficients in the Z bias correction were similar to all the rainfall types, typhoon cases had the lowest accuracy in the RMSE. As a result of the Z bias_MFBC, the correlation coefficients in all types were improved when compared with the Z bias. While the accuracy of the Z bias_MFBC in the RMSE improved over the Z bias, with the exception of the Changma front cases, the results of the typhoon cases were inferior to others as always. The results of the Z bias_LGC showed that the accuracy of the rainfall estimates for all types in the RMSE and the correlation coefficients was superior to the Z bias and, especially, the outcomes in the typhoon cases were vastly superior to the others. Figure 10 explains that the RMSEs of the Z bias_LGC of all cases were outstanding in Fig. 10a and, while the correlation coefficients of the Z bias_MFBC were not much different to the Z bias_LGC on average, only the Z bias correction results were generally lower in Fig. 10b.

Figure 11 shows the rainfall estimate images of the AWS, the Z bias, the Z bias_MFBC, and the Z bias_LGC in Case 12 (at 15:00 LST on 10 August 2012) and Case 18 (at 11:00 LST on 30 August 2012). In Fig. 10a in Case 12, the maximum rainfall amount in the AWSs was 48.0 mm h^{-1} , and the black arrows indicate the

Title Page

Abstract

Introduction

Conclusions

References

Tables

Figures

|◀

▶|

◀

▶

Back

Close

Full Screen / Esc

Printer-friendly Version

Interactive Discussion

strongest rainfall fields. Figure 11b shows that since the displayed rainfall regions were similar to the AWSs, the rainfall amounts were underestimated in the whole area. As an image of the Z bias_MFBC in Fig. 11c, the rainfall amounts in the black circle were closer to the AWSs than Fig. 11b. Especially, the image of the Z bias_LGC is similar to the AWSs and the rainfall estimates, which ranged from 40 to 50 mm h^{-1} in the regions (indicated by black arrows in a black circle), were similar to the AWSs. In Fig. 12a in Case 18, the maximum rainfall amount in the AWSs was 54.0 mm h^{-1} and the rainfall fields indicated by the black arrows were stronger than the others. Particularly, the rainfall zones (the black dash line) from the southwest to the northeast occurred due to the direct effects of Typhoon Tembin along its track (the purple line). Figure 12b shows that the rainfall amounts in only the Z bias were much underestimated in the whole area. By contrast, in Fig. 12c for the Z bias_MFBC, the maximum rainfall estimates in region ① (which was located in the southeast of the Tembin), and in the rainfall zones from the southwest to the northeast (region ②) were much improved. However, the rainfall estimates in region ① were a little underestimated, and region ② had slightly strong rainfall amounts. In Fig. 12d, since rainfall estimates in region ③ were stronger than for region ①, and region ④ had lighter rainfall amounts than region ②, an image of the rainfall estimates in the Z bias_LGC was coterminous with the AWSs. It is proven that the accuracy of the rainfall estimates in the RAR system, with the rainfall estimation bias correction, is improved compared to using only the Z bias correction in particular, the Z bias_LGC is superior to the others.

4 Conclusions

This paper focuses on correcting the reflectivity measurement bias (Z bias), which includes the temporal and spatial sampling bias, ground and sea clutter, beam-blockage and attenuation, electrical calibration, and quantification of the reflectivity bias and the rainfall estimation bias by the QPE model bias, which includes the bias resulting from the parameters of the Z – R relationship, the parameters of the QPE model,

[Title Page](#)[Abstract](#)[Introduction](#)[Conclusions](#)[References](#)[Tables](#)[Figures](#)[|◀](#)[▶|](#)[Back](#)[Close](#)[Full Screen / Esc](#)[Printer-friendly Version](#)[Interactive Discussion](#)

and the QPE model structure, to improve the radar rainfall estimates. The reference radar, a Bislsan S-band dual-polarimetric radar that was self-calibrated with the self-consistency constraint method (using the relationship between Z and K_{DP}) was utilized to calculate the Z biases of all target radar sites; the Z biases were applied to the QPE model with the RAR system. The MFBC and LGC methods, which correct rainfall estimation biases, have also been applied to the RAR system to improve the accuracy of the radar rainfall estimates.

As a result of the Z bias correction in 18 summer season cases, the accuracy of the rainfall estimates improved in the RMSE and the correlation coefficient (which ranged from 7.37 mm h^{-1} and 0.83 and 7.21 mm h^{-1} and 0.84 on average) and, for rainfall types, the accuracy of the rainfall estimates in the Changma front and local torrential cases were slightly improved or were similar to the results without the application of the Z bias. In particular, the accuracy of typhoon cases was worse than the existing results (from 9.08 to 11.04 mm h^{-1}). The reason for this is that the application of the Z biases to each radar site in the RAR system increased the rainfall estimates for the whole country. The accuracy of the Changma front cases, which occur nationwide, was improved; however, because cases of torrential rainfalls and typhoons have occurred locally, the accuracy of these cases was worse. In comparison with rainfall images, rainfall estimates with the Z bias correction have been established to be stronger than existing images.

Since the rainfall estimates in the RAR system have been improved by the Z bias correction, the rainfall estimation bias correction was conducted after the Z bias correction. For results of the rainfall estimation bias correction methods, the accuracy of the rainfall estimates with the Z bias_MFBC was improved by about 7.4 % in the RMSE and 10.7 % in the correlation coefficient, in comparison with only the Z bias, respectively; the accuracy of the Z bias_LGC was especially superior to the others (63.7 % in the RMSE and 11.7 % in the correlation coefficient). The reason for this is that, although the same rainfall estimation bias was applied to the allover area in the MFBC method, the different rainfall estimation biases were applied to each rainfall amount by the radar

[Title Page](#)[Abstract](#)[Introduction](#)[Conclusions](#)[References](#)[Tables](#)[Figures](#)[|](#)[|](#)[◀](#)[▶](#)[Back](#)[Close](#)[Full Screen / Esc](#)[Printer-friendly Version](#)[Interactive Discussion](#)

pixel in the LGC method. For the rainfall types, the results of the *Z* bias_LGC showed that the accuracy of the rainfall estimates for all types in the RMSE and the correlation coefficient was much improved over only the *Z* bias and, especially, the outcomes in the typhoon cases were vastly superior to the others. In a comparison of the rainfall images, the rainfall estimates with the *Z* bias_LGC were determined to be closer to the AWSs in the cases of the Changma fronts and Typhoon Tembin.

Therefore, in this paper, it is proven that the accuracy of the rainfall estimates in the RAR system, to which the *Z* bias correction and the rainfall estimation bias correction method (MFBC and LGC) were applied, has been improved. These bias correction methods proposed by this paper are able to contribute to the real-time QPE model, the RAR system, in the work-site operation and to the fundamental bias correction research. However, this paper has dealt with the bias corrections, in a few parts, in a procedure series. Since the radar rainfall estimates are still based on a series of assumptions, more research on numerous systematic biases, including natural biases, should undertake the calculation of radar-based rainfall estimates.

Acknowledgements. This research was supported by the Daejin University Research Grants in 2015.

References

Austin, P. M.: Relation between measured radar reflectivity and surface rainfall, *Mon. Weather Rev.*, 115, 1053–1070, 1987.

20 Campos, E. and Zawadzki, I.: Instrumental uncertainties in Z – R relations, *J. Appl. Meteorol.*, 39, 1088–1102, 2000.

Chumchean, S., Sharma, A., and Seed, A.: An integrated approach to error correction for real-time radar-rainfall estimation, *J. Atmos. Ocean. Tech.*, 23, 67–79, 2006.

25 Ehret, U.: Rainfall and flood nowcasting in small catchments using weather radar, PhD thesis, University of Stuttgart, Germany, 2002.

Germann, U., Galli, G., Boscacci, M., and Bolliger, M.: Radar precipitation measurement in a mountainous region, *Q. J. Roy. Meteor. Soc.*, 132, 1669–1692, 2006.

[Title Page](#)

[Abstract](#)

[Introduction](#)

[Conclusions](#)

[References](#)

[Tables](#)

[Figures](#)

[◀](#)

[▶](#)

[◀](#)

[▶](#)

[Back](#)

[Close](#)

[Full Screen / Esc](#)

[Printer-friendly Version](#)

[Interactive Discussion](#)



Huff, F. A.: Sampling errors in measurement of mean precipitation, *J. Appl. Meteorol.*, 9, 35–44, 1970.

Jeong, J., Yu, M., and Yi, J.: Runoff analysis using dual polarization radar and distributed model, *J. Korea Water Resour. Assoc.*, 47, 801–812, 2014.

5 Jordan, P., Seed, A., and Austin, G.: Sampling errors in radar estimates of rainfall, *J. Geophys. Res.-Atmos.*, 105, 2247–2257, 2000.

Kim, D.-S., Kang, M.-Y., Lee, D.-I., Kim, J.-H., Choi, B.-C., and Kim, K. E.: Reflectivity Z and differential reflectivity ZDR correction for polarimetric radar rainfall measurement, Proceeding of the Spring Meeting of Korean Meteorological Society, 10–11 April 2006, Gwangju, Korea, 10 130–131, 2006.

Kim, J.-B., Choi, W.-S., and Bae, D.-H.: Assessment of dual-polarization radar for flood forecasting, *J. Korea Water Resour. Assoc.*, 48, 257–268, 2015.

Korea Meteorological Administration: Development of collaboration management system for radar data (I). Weather Radar Center, Korea Meteorological Administration, Weather Radar Center, Korea, 2011.

15 Korea Meteorological Administration: Development of Radar-based Multi-sensors Quantitative Precipitation Estimation Technique Report, Weather Radar Center, Korea Meteorological Administration, Weather Radar Center, Korea, 2012a.

Korea Meteorological Administration: Radar rainfall estimation comparison and verification joint 20 experiment report. Weather Radar Center and Meteorological Advancement Council, Korea Meteorological Administration, 2012b.

Krajewski, W. F. and Smith, J.: Radar hydrology: rainfall estimation, *Adv. Water Resour.*, 25, 1387–1394, 2002.

Lee, G. W.: Sources of errors in rainfall measurements by polarimetric radar: variability of drop 25 size distributions, observational noise, and variation of relationships between R and polarimetric parameters, *J. Atmos. Ocean. Tech.*, 23, 1005–1028, 2006.

Marshall, J. S. and Palmer, W. M.: The distribution of raindrops with size, *J. Meteorol.*, 5, 165–166, 1948.

McMillan, H., Jackson, B., Clark, M., Kavetski, D., and Woods, R.: Rainfall uncertainty in hydrological modeling: an evaluation of multiplicative error models, *J. Hydrol.*, 400, 83–94, 2011.

30 Morin, E. and Gabella, M.: Radar-based quantitative precipitation estimation over Mediterranean and dry climate regimes, *J. Geophys. Res.*, 112, D20108, doi:10.1029/2006JD008206, 2007.

Application of bias correction methods to improve quantitative radar rainfall in Korea

J.-K. Lee et al.

[Title Page](#)

[Abstract](#)

[Introduction](#)

[Conclusions](#)

[References](#)

[Tables](#)

[Figures](#)

[◀](#)

[▶](#)

[◀](#)

[▶](#)

[Back](#)

[Close](#)

[Full Screen / Esc](#)

[Printer-friendly Version](#)

[Interactive Discussion](#)



Moulin, L., Gaume, E., and Obled, C.: Uncertainties on mean areal precipitation: assessment and impact on streamflow simulations, *Hydrol. Earth Syst. Sci.*, 13, 99–114, doi:10.5194/hess-13-99-2009, 2009.

5 Oh, H.-M., Ha, K.-J., Kim, K.-E., and Bae, D.-H.: Precipitation rate combined with the use of optimal weighting of radar and rain gauge data, *Atmosphere*, Korean Meteorol. Soc., 13, 316–317, 2003.

Rosenfeld, D., Wolff, D. B., and Atlas, D.: General probability-matched relations between radar reflectivity and rain rate, *J. Appl. Meteorol.*, 32, 50–72, 1993.

10 Sinclair, S. and Pegram, G.: Combining radar and rain gauge rainfall estimates using conditional merging, *Atmos. Sci. Lett.*, 6, 19–22, 2005.

Villarini, G.: Empirically-based modeling of radar-rainfall uncertainties, PhD thesis, The University of Iowa, USA, 321, 2008.

15 Villarini, G. and Krajewski, W. F.: Empirically-based modeling of spatial sampling uncertainties associated with rainfall measurements by rain gauges, *Adv. Water Resour.*, 31, 1015–1023, 2008.

Villarini, G. and Krajewski, W. F.: Sensitivity studies of the models of radar-rainfall uncertainties, *J. Appl. Meteorol. Clim.*, 49, 288–309, 2010.

20 Villarini, G., Mandapaka, P. V., Krajewski, W. F., and Moore, R. J.: Rainfall and sampling errors: a rain gauge perspective, *J. Geophys. Res.*, 113, D11102, doi:10.1029/2007JD009214, 2008.

Weather Radar Center: Development of integrated quality control algorithm for Korean radar data, Korea Meteorological Administration, Weather Radar Center, Korea, 2013.

25 Wilson, J. W. and Brandes, E. A.: Radar measurement of rainfall, *B. Am. Meteorol. Soc.*, 60, 1048–1058, 1979.

Woodley, W., Olsen, A., Herndon, A., and Wiggert, V.: Comparison of gage and radar methods of convective rain measurement, *J. Appl. Meteorol.*, 14, 909–928, 1975.

30 Yoo, C., Kim, J., Yoon, J., Park, C., Park, C., and Jun, C.: Use of the Kalman filter for the correction of mean-field bias of radar rainfall, The 5th Korea-Japan-China Joint Conference on Meteorology, Busan, Korea, 24–26 October 2011, p. 277, 2011.

You, C.-H., Lee, D.-I., and Kang, M.-Y.: Rainfall estimation using specific differential phase for the first operational polarimetric radar in Korea, *Adv. Meteorol.*, 2014, 413717, doi:10.1155/2014/413717, 2014.

Application of bias correction methods to improve quantitative radar rainfall in Korea

J.-K. Lee et al.

[Title Page](#)

[Abstract](#)

[Introduction](#)

[Conclusions](#)

[References](#)

[Tables](#)

[Figures](#)

[◀](#)

[▶](#)

[◀](#)

[▶](#)

[Back](#)

[Close](#)

[Full Screen / Esc](#)

[Printer-friendly Version](#)

[Interactive Discussion](#)

Zhang, J., Howard, K., Langston, C., Vasiloff, S., Kaney, B., Arthur, A., Cooten, V. C., Kelleher, K., Kitzmiller, D., Ding, F., Seo, D.-J., Wells, E., and Dempsey, C.: National mosaic and multi-sensor QPE(NMQ) system: description, results, and future plans, *B. Am. Meteorol. Soc.*, 92, 1321–1338, 2011.

5 Zhang, Y., Adams, T., and Bonta, J. V.: Subpixelscale rainfall variability and the effects on the separation of radar and gauge rainfall errors, *J. Hydrometeorol.*, 8, 1348–1363, 2007.

Application of bias correction methods to improve quantitative radar rainfall in Korea

J.-K. Lee et al.

Title Page	
Abstract	Introduction
Conclusions	References
Tables	Figures
◀	▶
◀	▶
Back	Close
Full Screen / Esc	

Printer-friendly Version
Interactive Discussion

Table 1. (a) A summary of the radars and rainfall cases. Summary of the radars and rainfall data used for calculating observational biases. **(b)** Rainfall cases used for verification of the observational and model bias correction.

(a) Items	Details
Reference radar	Bislsan S-band dual-polarization radar (Maximum observation range: 150 km; Gate size: 0.125 km; Elevation: 6 angles; Update: every 2.5 min interval)
Target radar	11 single-polarization radars operated by the Korea Meteorological Administration: Baegnyeondo (BRI, S-band), Kwanaksan (KWK, S-band), Oseon-san (KSN, S-band), Jindo (JNI, S-band), Gosan (GSN, S-band), Seongsan (SSP, S-band), Gudeoksan (PSN, S-band), Myeon-bongsan (MYN, C-band), Gangneung (GNG, S-band), Gwnagdeok-san (GDK, S-band), Incheon (IIA, C-band)
Calibration data	Rainfall cases from 1 Jun to 31 Aug in 2012

(b) Items	Period (LST)	Sources
Case 1	8 Jun 2012, 06:00–8 Jun 2012, 19:00	Local torrential rainfalls
Case 2	15 Jun 2012, 05:00–16 Jun 2012, 04:00	Changma front
Case 3	18 Jun 2012, 00:00–19 Jun 2012, 13:00	Changma front
Case 4	23 Jun 2012, 13:00–24 Jun 2012, 19:00	Local torrential rainfalls
Case 5	29 Jun 2012, 08:00–1 Jul 2012, 01:00	Changma front
Case 6	5 Jul 2012, 04:00–7 Jul 2012, 02:00	Changma front
Case 7	10 Jul 2012, 10:00–11 Jul 2012, 19:00	Changma front
Case 8	12 Jul 2012, 23:30–13 Jul 2012, 07:30	Changma front
Case 9	14 Jul 2012, 08:00–15 Jul 2012, 15:00	Changma front
Case 10	16 Jul 2012, 23:00–17 Jul 2012, 22:00	Changma front
Case 11	18 Jul 2012, 14:00–19 Jul 2012, 13:00	Typhoon
Case 12	10 Aug 2012, 03:00–10 Aug 2012, 22:00	Local torrential rainfalls
Case 13	12 Aug 2012, 05:00–13 Aug 2012, 15:00	Local torrential rainfalls
Case 14	14 Aug 2012, 17:00–16 Aug 2012, 23:00	Local torrential rainfalls
Case 15	19 Aug 2012, 16:00–22 Aug 2012, 21:00	Local torrential rainfalls
Case 16	22 Aug 2012, 22:00–25 Aug 2012, 11:00	Local torrential rainfalls
Case 17	27 Aug 2012, 13:00–28 Aug 2012, 18:00	Changma front and Typhoon
Case 18	29 Aug 2012, 15:00–30 Aug 2012, 23:00	Typhoon

Table 2. The radar pairs for estimating the Z bias of each radar site.

Reference radar	Target radar	Reference radar	Target radar
BSL	KSN, PSN, MYN	IIA	BRI
KSN	JNI	KSN	KWK
JNI	GSN, SSP	KWK	GDK
KWK	IIA	GDK	GNG

Title Page	
Abstract	Introduction
Conclusions	References
Tables	Figures
◀	▶
◀	▶
Back	Close
Full Screen / Esc	
Printer-friendly Version	
Interactive Discussion	

Table 3. The reflectivity bias for each radar site.

Radar site	Reflectivity bias (dB)	Radar site	Reflectivity bias (dB)
BRI	-7.87*	JNI	-1.16
GDK	-4.29	KSN	-4.87
GSN	-3.99	KWK	-5.15
GNG	-4.77	MYN	-5.63
IIA	-5.19	PSN	-2.28
SSP	-4.50		

* Average reflectivity bias during the calibration period.

[Title Page](#) [Abstract](#) [Introduction](#) [Conclusions](#) [References](#) [Tables](#) [Figures](#) [◀](#) [▶](#) [◀](#) [▶](#) [Back](#) [Close](#) [Full Screen / Esc](#)

[Printer-friendly Version](#) [Interactive Discussion](#)



Table 4. (a) The application results of the rainfall estimation bias correction methods. Total average. (b) Average for each rainfall type.

(a) Method	MAE (mm h^{-1})	RMSE (mm h^{-1})	Correlation coefficient
Z bias	3.65	7.21	0.84
Z bias_MFBC	3.37	6.68 (7.4 %*)	0.93 (10.7 %)
Z bias_LGC	2.19	2.62 (63.7 %)	0.94 (11.7 %)

(b) Method	Types	Averaged RMSE (mm h^{-1})	Averaged correlation coefficient
Z bias	Changma front	5.64	0.87
	Local torrential rainfall	7.36	0.81
	Typhoon	11.04	0.83
Z bias_MFBC	Changma front	5.75	0.93
	Local torrential rainfall	6.74	0.95
	Typhoon	9.00	0.86
Z bias_LGC	Changma front	2.49	0.95
	Local torrential rainfall	2.69	0.94
	Typhoon	2.81	0.93

* Represents the change ratio related to the OBC method in RMSE and correlation coefficient.

Application of bias correction methods to improve quantitative radar rainfall in Korea

J.-K. Lee et al.

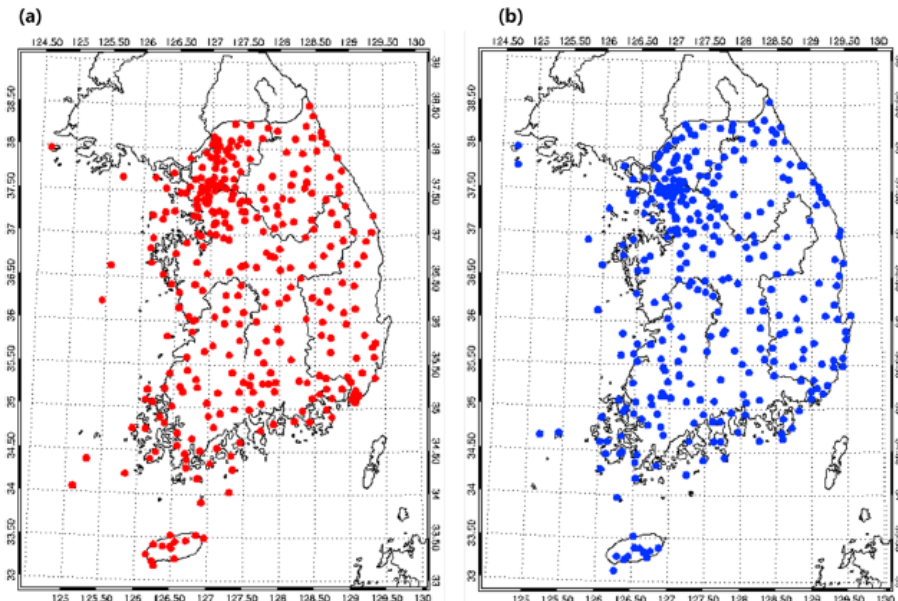


Figure 1. Locations of 642 observation rain gauges: **(a)** 321 rain gauge locations for the calibration, **(b)** 321 rain gauge locations for the validation.

[Title Page](#)

[Abstract](#)

[Introduction](#)

[Conclusions](#)

[References](#)

[Tables](#)

[Figures](#)

◀

▶

◀

▶

[Back](#)

[Close](#)

[Full Screen / Esc](#)

[Printer-friendly Version](#)

[Interactive Discussion](#)

Application of bias correction methods to improve quantitative radar rainfall in Korea

J.-K. Lee et al.

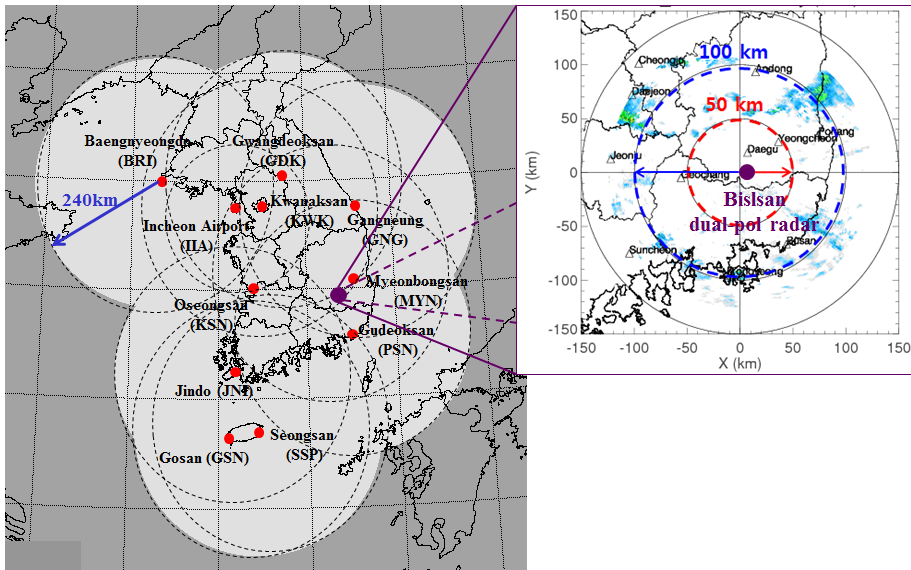


Figure 2. The location of 11 single-polarization radars and the Bislsan S-band dual-polarization radar and their observation ranges.

[Title Page](#)

[Abstract](#)

[Introduction](#)

[Conclusions](#)

[References](#)

[Tables](#)

[Figures](#)

[|◀](#)

[▶|](#)

[◀](#)

[▶](#)

[Back](#)

[Close](#)

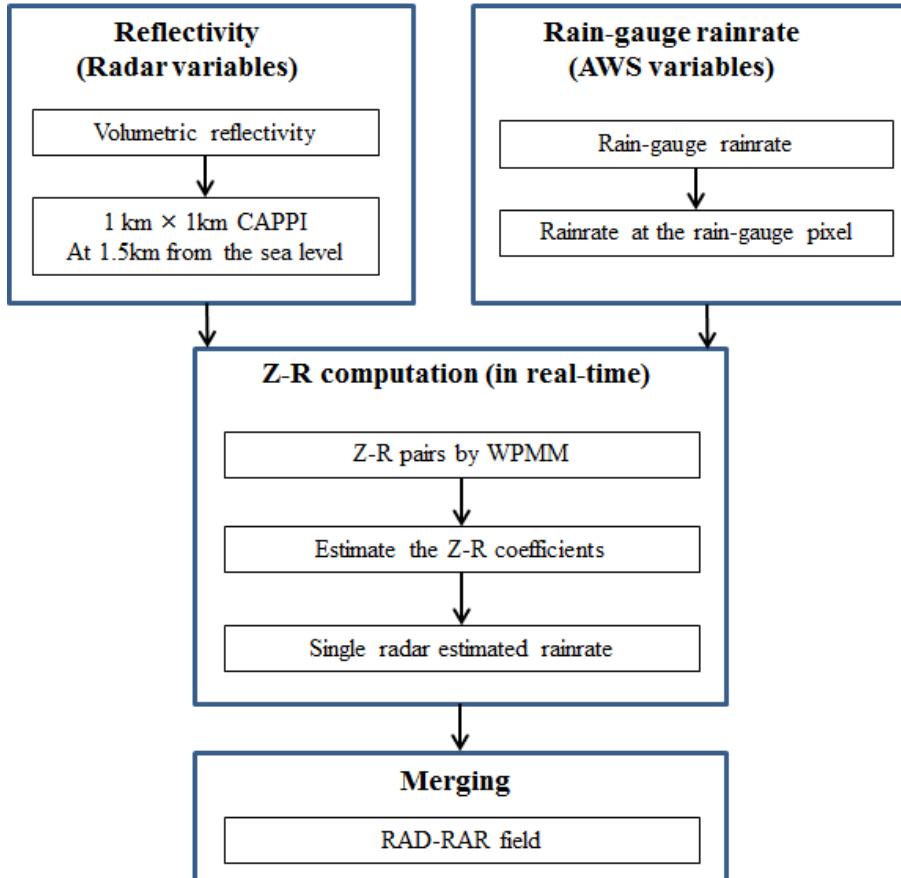
[Full Screen / Esc](#)

[Printer-friendly Version](#)

[Interactive Discussion](#)

Application of bias correction methods to improve quantitative radar rainfall in Korea

J.-K. Lee et al.

**Figure 3.** A flowchart of the Radar-AWS Rainrate calculation system.

Application of bias correction methods to improve quantitative radar rainfall in Korea

J.-K. Lee et al.

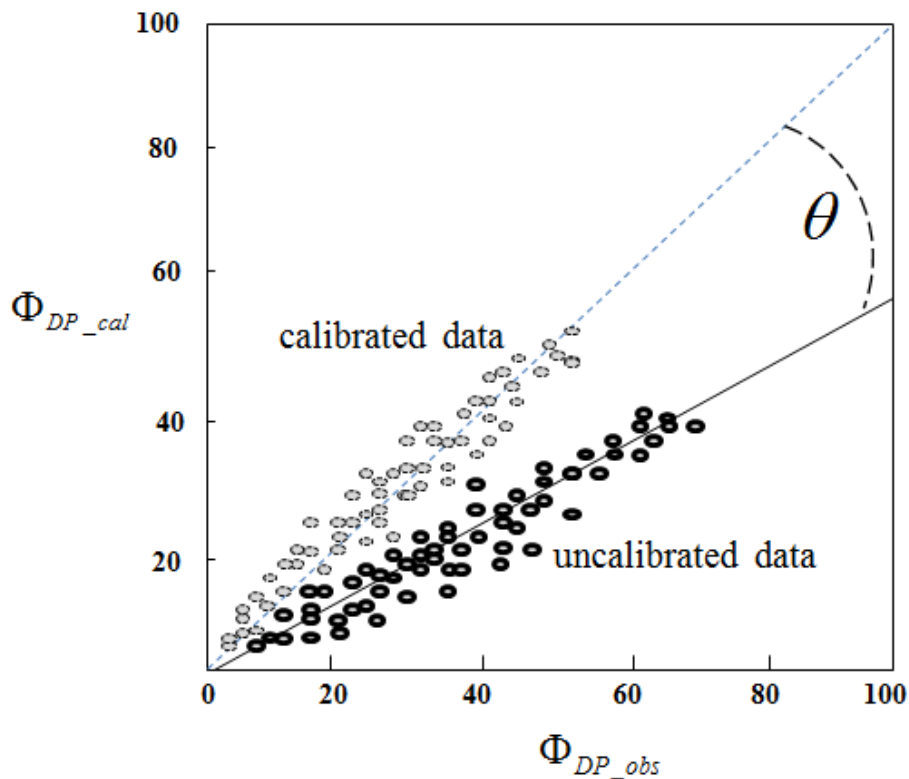


Figure 4. Example for the procedure of the self-consistency constraint: calculation of $\tan \theta$ using Eq. (3).

Title Page	Abstract	Introduction
Conclusions	References	
Tables	Figures	
◀	▶	
◀	▶	
Back	Close	
Full Screen / Esc		
Printer-friendly Version		
Interactive Discussion		

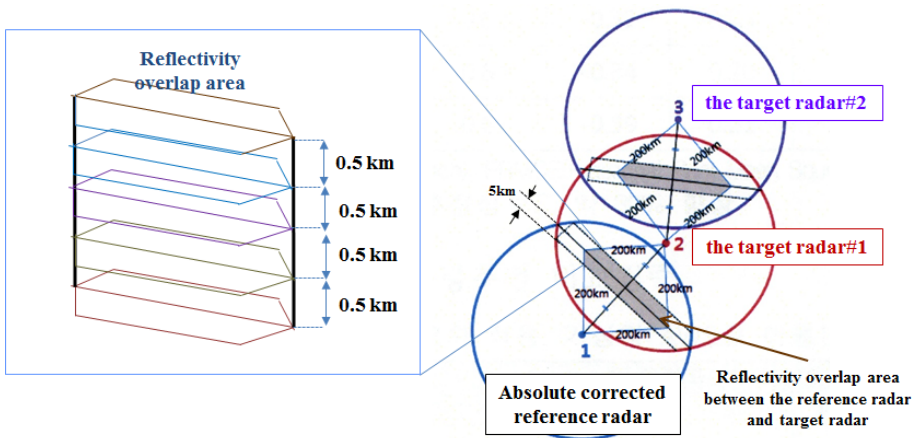


Figure 5. The concept of calculating Z bias for the target radar according to the reference radar reflectivity (Korea Meteorological Administration, 2011).

Application of bias correction methods to improve quantitative radar rainfall in Korea

J.-K. Lee et al.

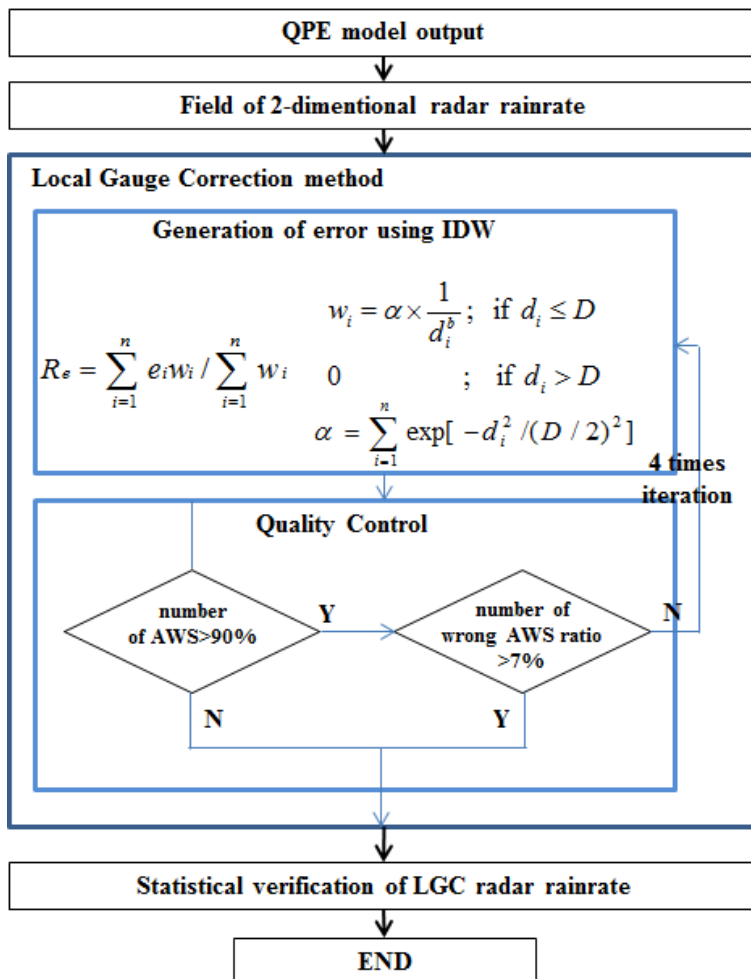


Figure 6. A Flowchart of the Local Gauge Correction method.

**Application of bias correction methods
to improve
quantitative radar
rainfall in Korea**

J.-K. Lee et al.

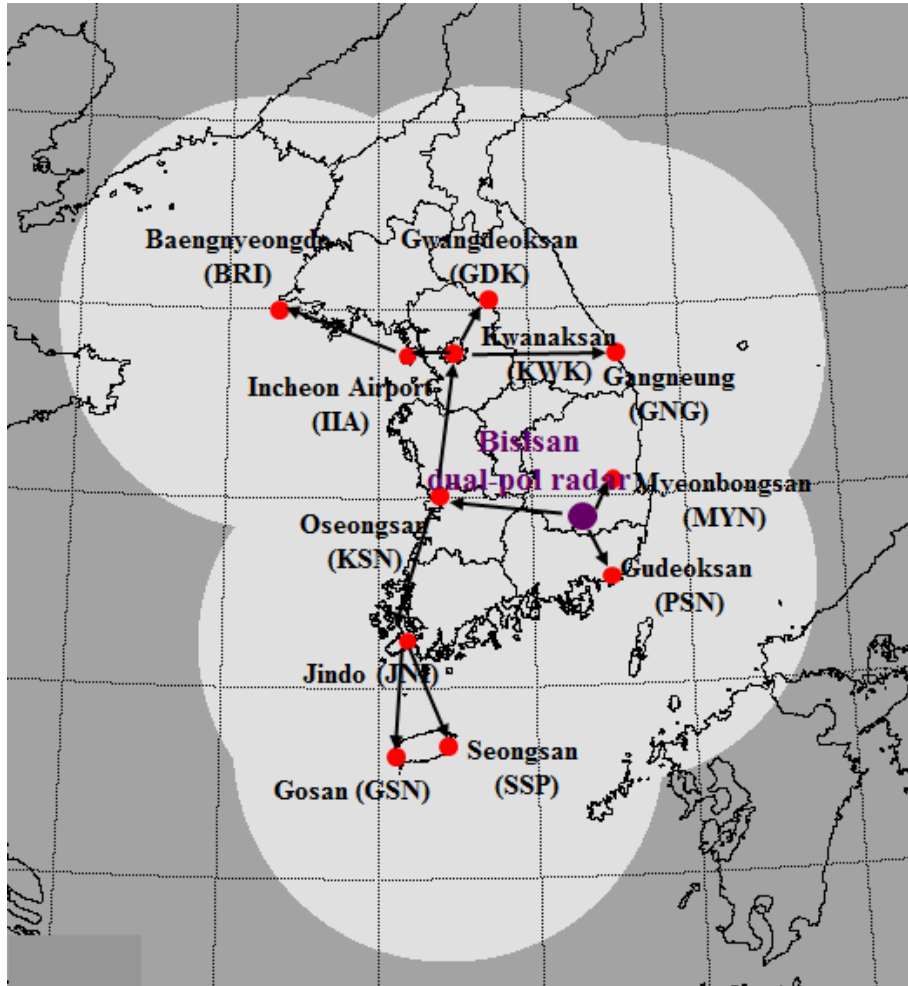


Figure 7. The Sequence of the reflectivity bias estimation for each radar site.

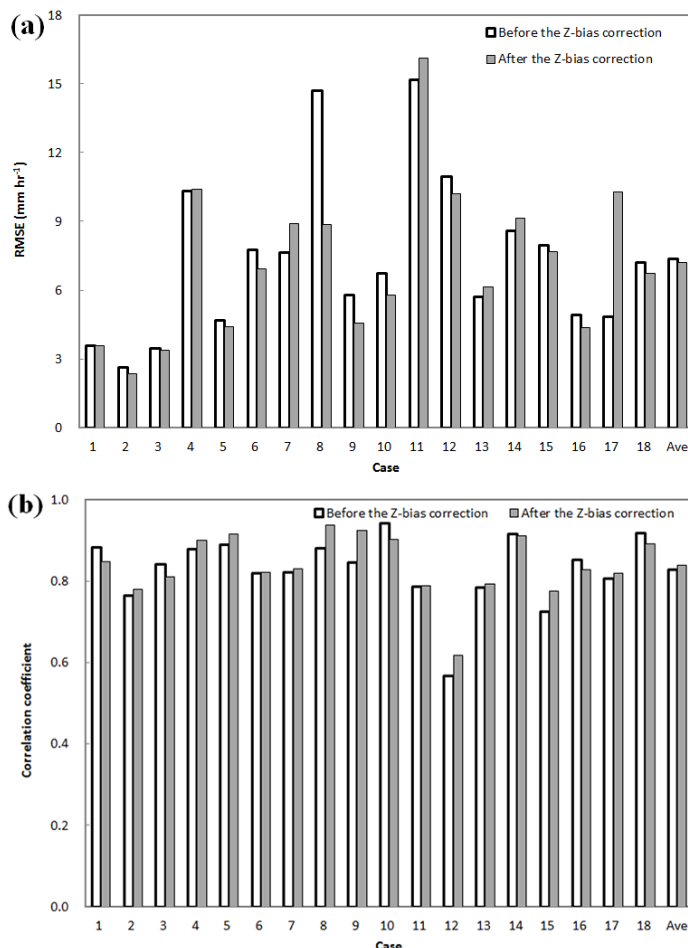


Figure 8. A comparison of the accuracy of rainfall estimates for each rainfall case before and after the Z bias correction: **(a)** RMSE; **(b)** correlation coefficient.

Application of bias correction methods to improve quantitative radar rainfall in Korea

J.-K. Lee et al.

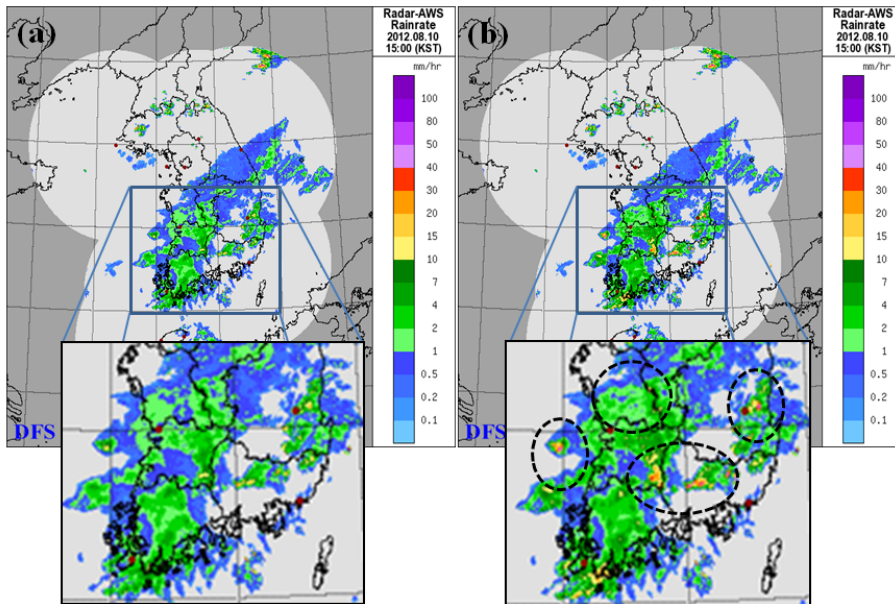


Figure 9. A comparison of rainfall estimate images in the RAR system before and after the Z bias correction in Case 12 (at 15:00 LST on 10 August in 2012): **(a)** before the Z bias correction; **(b)** after the Z bias correction.

Title Page

Abstract

Introduction

Conclusions

References

Tables

Figures

1

A small, light blue rectangular button with a white right-pointing triangle icon, located in the bottom right corner of the slide.

Back

Close

Full Screen / Esc

Interactive Discussion

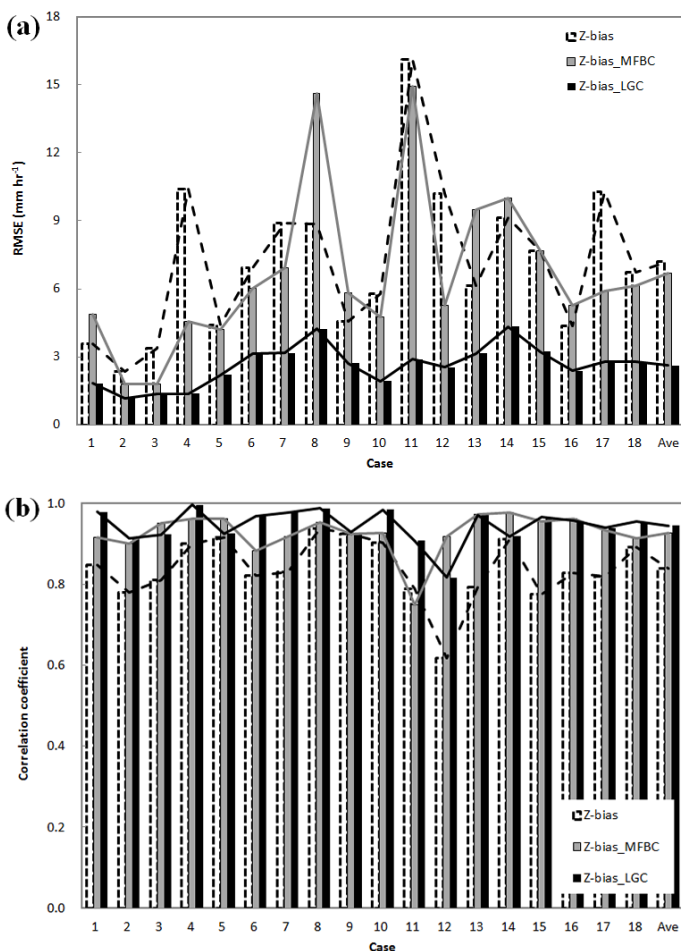


Figure 10. A comparison of the rainfall estimation accuracy for each rainfall in the Z bias, Z bias MFBC, and Z bias LGC methods: **(a)** RMSE; **(b)** correlation coefficient.

Application of bias correction methods to improve quantitative radar rainfall in Korea

J.-K. Lee et al.

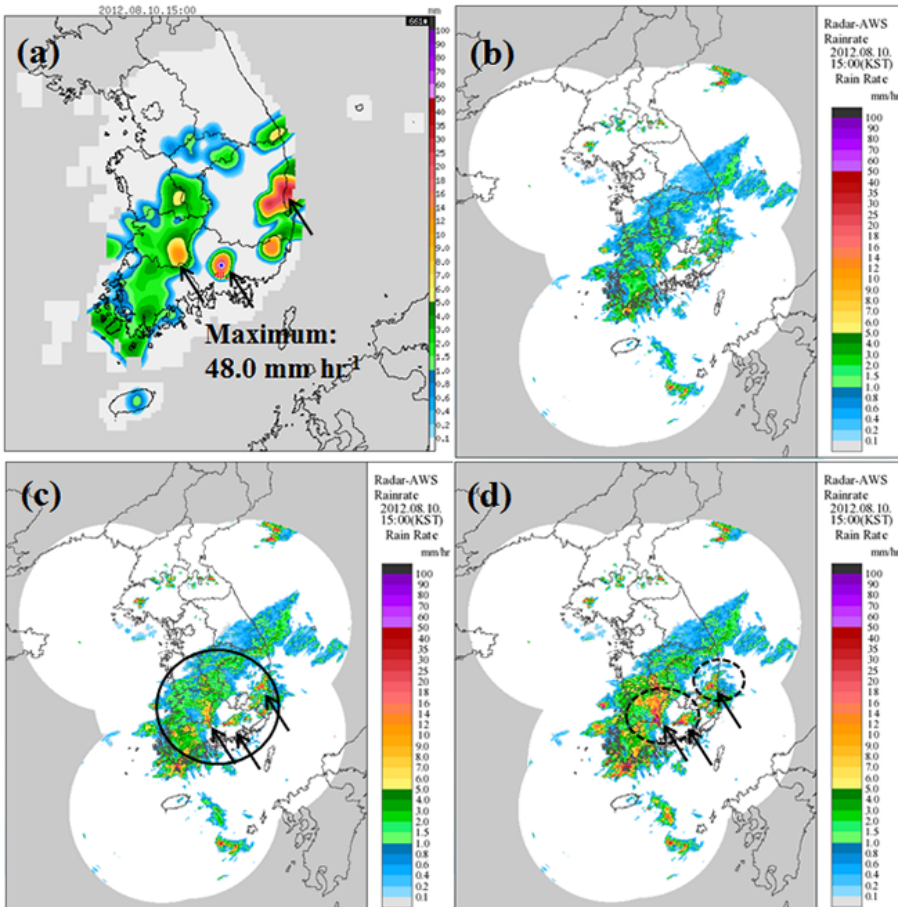


Figure 11. A comparison of the rainfall images between the AWS and rainfall estimation bias correction method results in Case 12 (at 15:00 LST on 10 August in 2012): **(a)** the AWS; **(b)** the OBC method; **(c)** the OBC_MFBC method; **(d)** the OBC_LGC method.

Application of bias correction methods to improve quantitative radar rainfall in Korea

J.-K. Lee et al.

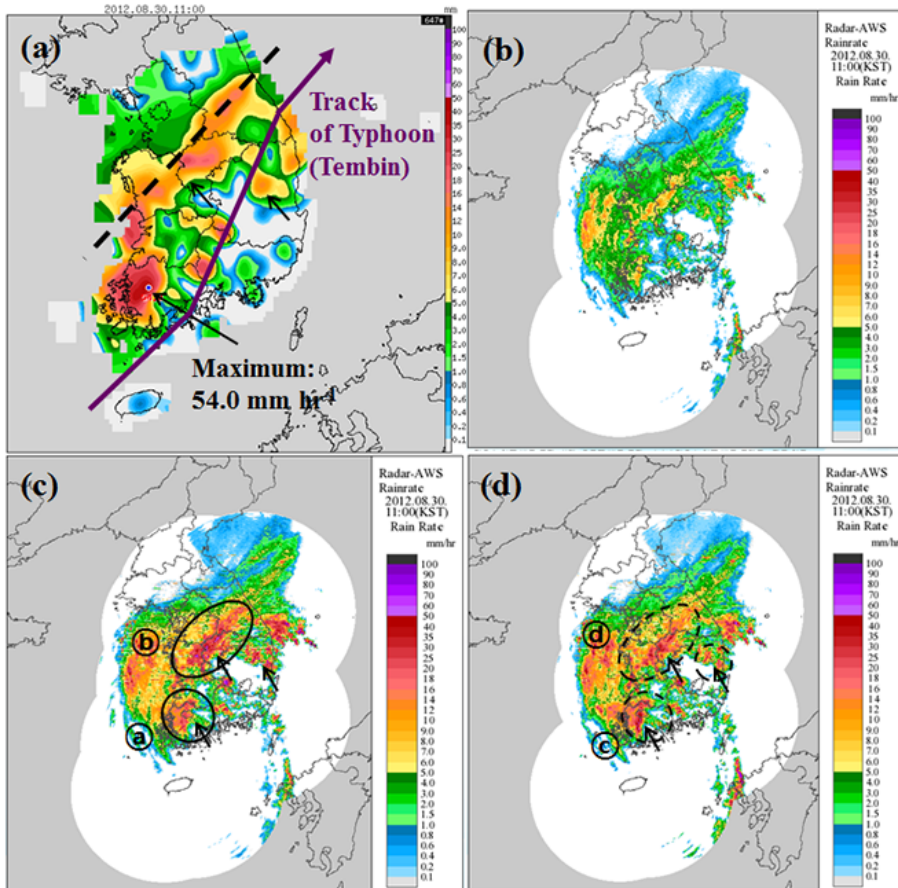


Figure 12. A comparison of the rainfall images between the AWS and rainfall estimation bias correction method results in Case 18 (at 11:00 LST on 30 August in 2012): **(a)** the AWS; **(b)** the OBC method; **(c)** the OBC_MFBC method; **(d)** the OBC_LGC method.